Time-differential perturbed-angular-correlation study of ^{111}In-^{111}Cd in III-V compounds

A. F. Pasquevich
Departamento de Fisica, Universidad Nacional de La Plata, Casilla de Correo No. 67, 1900 La Plata, Argentina

R. Vianden
Institut für Strahlen- und Kernphysik der Universität Bonn, 5300 Bonn, Federal Republic of Germany
(Received 16 October 1989)

The hyperfine interactions of ^{111}Cd in GaP, GaAs, GaSb, AlSb, and InSb were determined by means of the time-differential perturbed-angular-correlation technique. Doping with ^{111}Cd was achieved by ion implantation of the parent radioactive atom ^{111}In. After removal of radiation damage by thermal annealing the hyperfine interactions were studied in the temperature range 20–300 K. The results are compared with those of similar experiments recently reported for diamond-structure semiconductors and are also explained in terms of a distorted configuration of atoms surrounding the probe ion where holes may be bound. In addition, radiation-damage characteristics, thermal-annealing behavior, evidence of nonstoichiometry in GaSb, and the temperature dependence of the quadrupole interaction of probes in both gallium- and antimony-rich phases are discussed.

I. INTRODUCTION

In recent years the time-differential perturbed-angular-correlation (TDPAC) technique has been applied to study the hyperfine interactions of ^{111}Cd in the diamond-structure semiconductors Si (Refs. 1–3) and Ge.[4] In all these cases, cadmium was introduced into the host lattice by ion implantation of ^{111}In, which decays to the probe ion ^{111}Cd by electron capture. After removal of the radiation damage, the TDPAC spectra depend strongly on temperature, in spite of the cubic symmetry at lattice sites. In Si, this fact has been attributed by Deicher *et al.*[2] to "after effects" of the electron-capture decay. On the other hand, Kemerink *et al.*[3] assigned the hyperfine interactions observed in high-resistivity silicon to a Jahn-Teller distortion. We have ascribed the existence of static quadrupole interactions to the presence of electronic holes more or less strongly bound to the radioactive acceptor ion. Due to the low temperature where changes take place, we have connected the holes bound to the impurity with an A^+ center. Recent experiments[5] have been also explained by the presence of holes bound to the Cd acceptor while the temperature dependence of the electric field gradient (EFG) has been understood on the basis of a splitting of the Cd ground state and thermally activated population of these substates.

Trying to clarify what is the source of these interactions, we extended the experiments to ^{111}In implanted in germanium[4] and observed a fluctuating interaction at substitutional sites in this semiconductor in contrast to the static interactions that have been found in silicon.[1,2] The fluctuating interaction is ascribed to transitions between the locally distorted configuration around the probe ion. We have described the distorted configuration as a cloud of atoms slightly displaced from their lattice sites with electronic holes bound to this complex. It seems not to be possible at present to better describe the distorted configuration.

The difference between the results obtained for Si and Ge could be explained by taking into account the different physical properties of both hosts. We assume that the distorted configurations around the cadmium probes are qualitatively similar in both materials, but equivalent distortions are possibly separated by higher energy barriers in the former case. This can be expected, because the cohesive forces are weaker in Ge than in Si as is reflected in the values of melting point, lattice parameter, hardness, etc. In the case of bound electronic holes the same trend can be expected for the values of minimum energy gap, hole mobility, cadmium impurity levels, etc. The variation of the physical properties with increasing atomic number of the host atoms reflects the weakening of the bonds between the valence electrons and the atomic nuclei.[6]

A similar behavior is expected with increasing mean atomic number in III-V compounds. These semiconductors have the cubic sphalerite (zinc-blende) structure, which, like the diamond structure, consists of two interpenetrating face-centered cubic lattices, each occupied by one type of ion. The physical properties of the III-V compounds spread over a range which covers that of the elemental semiconductors. So, these compounds seem to be appropriate to investigate how the distorted configuration around the cadmium probe depends on the physical properties of the host lattice. It should be noted that indium, as an element of group III, after implantation and annealing, occupies the group-III sublattice and therefore cadmium behaves as a single acceptor in the III-V compounds whereas it is a double acceptor in group-IV lattices. On the other hand, ion implantation in III-V compounds produces stoichiometric disturbances because of the different scattering cross sections of the projectile and the two substrate constituents.[7]

We report here on experiments carried out on some III-V compounds, namely GaP, GaAs, GaSb, InSb, and AlSb. The experimental method is described in Sec. II

TABLE I. Characteristics of the materials, annealing treatments, and implantation profiles.

Host	Z	Purity (at. %)	Annealing Temperature (°C)[a]	Range (Å)	Straggling (Å)
GaP	23	99.999 9	650	365	144
GaAs	32	99.999	650	269	122
AlSb	32	99.5	650	364	171
GaSb	41	99.99	550	284	141
InSb	50	99.99	350	277	145

[a]Annealing time 30 min.

and the experimental results are shown in Sec. III. The existence of nonstoichiometry in some compounds and the anomalous behavior of some others is discussed in Sec. IV. Finally, the evidence for the existence of a distorted configuration around the cadmium probes at low temperature is discussed.

II. EXPERIMENTAL

A. Sample preparation

The samples were prepared by implanting 80 keV ^{111}In ions into polycrystalline III-V compounds. In all the cases the dose was $<10^{13}$ ions/cm^2. The purities of the materials used are listed in Table I. The projected range of the ions and the straggling are also shown.

After implantation the samples were encapsulated in quartz tubes and annealed in a vacuum ($p \leq 10^{-5}$ kPa). The thermal-annealing treatment was carried out at different temperatures on account of the different melting points of the host materials (Table I).

B. Data acquisition and treatment

The TDPAC measurements were performed through the well-known 171–247 keV γ-γ cascade of ^{111}Cd emitted after the electron-capture decay of ^{111}In. Coincidences between the rays were detected with a conventional four NaI(Tl) detector TDPAC apparatus. After subtraction of accidental coincidences, time spectra corresponding to angles 90° and 180° were combined to form the ratio

$$R(t)=2\frac{N(180°,t)-N(90°,t)}{N(180°,t)+2N(90°,t)} \sim A_2 G_2(t) , \quad (1)$$

A_2 being the experimental anisotropy and $G_2(t)$ the perturbation factor containing the relevant information about the hyperfine interaction.

C. Perturbation factors

If the perturbation is caused by a static EFG acting on the probe nucleus of quadrupole moment Q and the EFG tensor is described by its main component V_{zz} and the asymmetry parameter η, the perturbation factor is

$$G_2(t)=\sum_{n=0}^{3} s_n \cos(n\omega_n)\exp(-\delta\omega_n^2 t^2) . \quad (2)$$

The frequencies ω_n are related to the quadrupole interaction frequency $\nu_Q = eQV_{zz}/h$ by the relation $\omega_n = F_n(\eta)\nu_Q$. F_n and the coefficients s_n are known[8] functions of η. The exponential function accounts for a Gaussian frequency distribution.

If the perturbation is produced by an EFG which fluctuates and the fluctuations have a correlation time $\tau_c \ll \langle\omega^2\rangle^{-1/2}$ ($\langle\omega^2\rangle^{1/2}$ being the average interaction frequency), $G_2(t)$ is given by the Abragam and Pound[9]

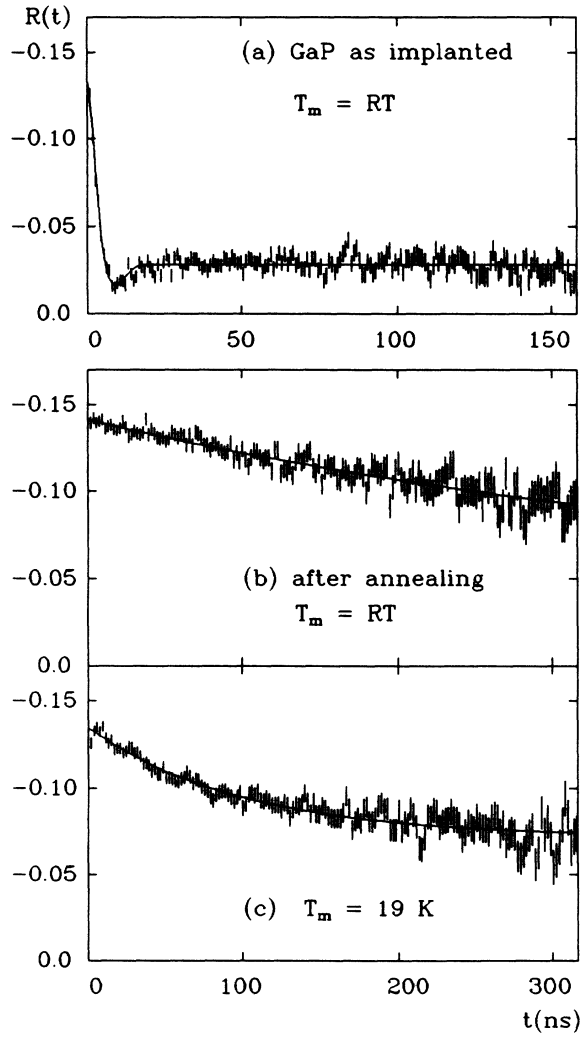

FIG. 1. TDPAC spectra of indium-implanted GaP (a) as implanted; (b) after annealing, measured at room temperature; and (c) after annealing, measured at 19 K.

TABLE II. Hyperfine parameters obtained for samples as implanted. For comparison also the results for Si (Ref. 1) and Ge (Ref. 4) are shown.

	$f_1(\%)$	ω_1 (Mrad/s)	δ_1	$f_2(\%)$	ω_2 (Mrad/s)	δ_2
GaP	100	44_1	0.63_2			
AlSb	94_4	31_1	0.51_1	6_1	1_1	0.0
GaAs	100	26_2	1.21_{20}			
GaSb	93_3	33_1	0.66_3	7_1	0	0.0
InSb	71_3	3_1	0.74_3	29_3	14_1	0.50_8
Si	91_3	31_1	0.77_5	9_1	71_1	0.04_4
Ge	68_{14}	34_6	0.72_2	32_{14}	77_2	0.19_4

limit

$$G_2(t)=\exp(-\lambda t)\ , \tag{3}$$

where λ is proportional to $\langle\omega^2\rangle\tau_c$.

III. RESULTS

A. GaP

The spectra obtained for In in GaP are shown in Fig. 1. The spectrum obtained with the sample "as implanted" [Fig. 1(a)] is well described with the perturbation factor given by Eq. (2). The values of the frequency distribution δ and the frequency ω_Q are given in Table II.

After annealing, the spectra are well fitted with the expression

$$G_2(t)=f_0+f_1\exp(-\lambda t)\ . \tag{4}$$

In the low-temperature range ($T<100$ K) $f_0=53\%$ and $f_1=47\%$. The parameter λ is shown as a function of temperature in Fig. 2. At room temperature the amplitudes f_0 and f_1 are different, but due to the small value of λ both parameters are strongly correlated, so that it is difficult to estimate what importance should be attributed to this fact.

The presence of two components can be ascribed to the existence of two types of regions where the probes are localized in GaP. In one zone, the probes do not trap holes and no distortion occurs. The existence of two regions with different properties can be explained by differences in stoichiometry. One region would be p type and the other one, n type. Both zones can result from the stoichiometric disturbances produced by the implantation process. These disturbances are greater in the present case due to the different masses of both constitu-

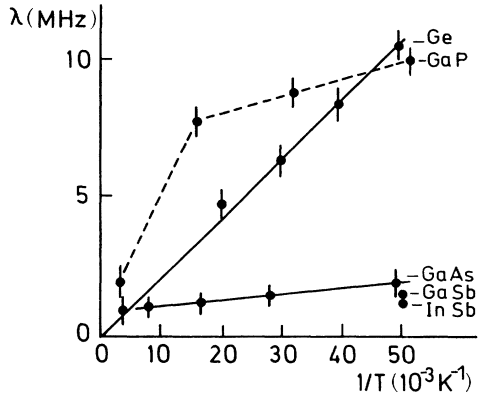

FIG. 2. The relaxation parameter λ is shown as a function of the temperature for all compounds studied. Data for Ge are also included for comparison. The data of GaSb and InSb are only shown at the lowest measurement temperature. The lines are only to guide the eyes.

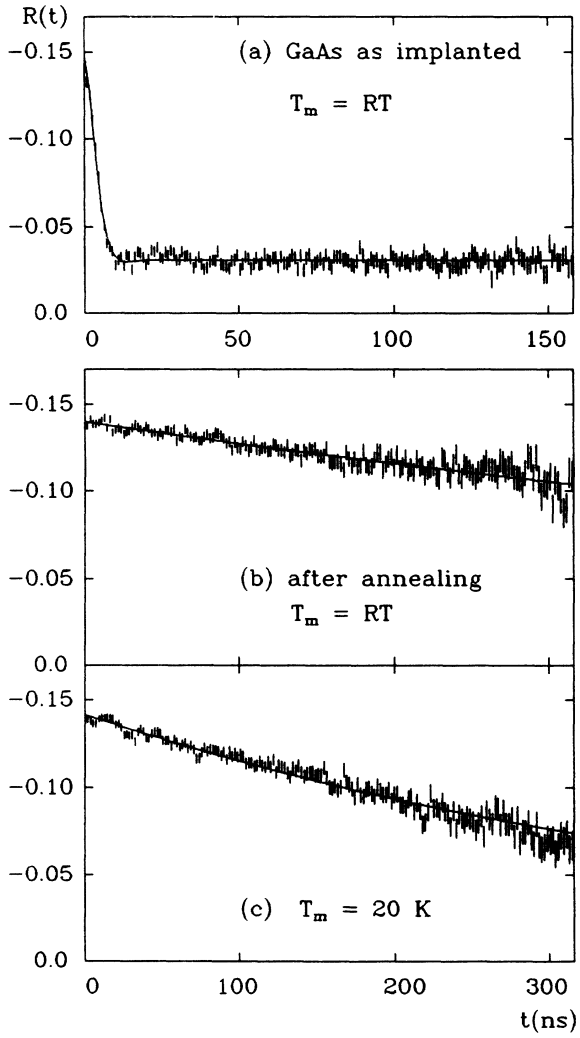

FIG. 3. TDPAC spectra of indium-implanted GaAs (a) as implanted; (b) after annealing, measured at room temperature; and (c) after annealing, measured at 20 K.

ents. In addition, the annealing treatment is another source of stoichiometry deviation.

The parameter λ takes values similar to those observed in germanium (also shown in Fig. 2 for comparison.) The present results are qualitatively similar to those reported for ^{111}Cd in InP.[10]

B. GaAs

Typical spectra obtained for GaAs are shown in Fig. 3. The spectrum "as implanted" is described with expression (2) and the values of the interaction parameters are given in Table II. The spectra obtained after annealing can be fitted with Eq. (4) but in this case only one probe site is found. There is not an unperturbed component. The relaxation parameter λ is shown in Fig. 2 as a function of temperature.

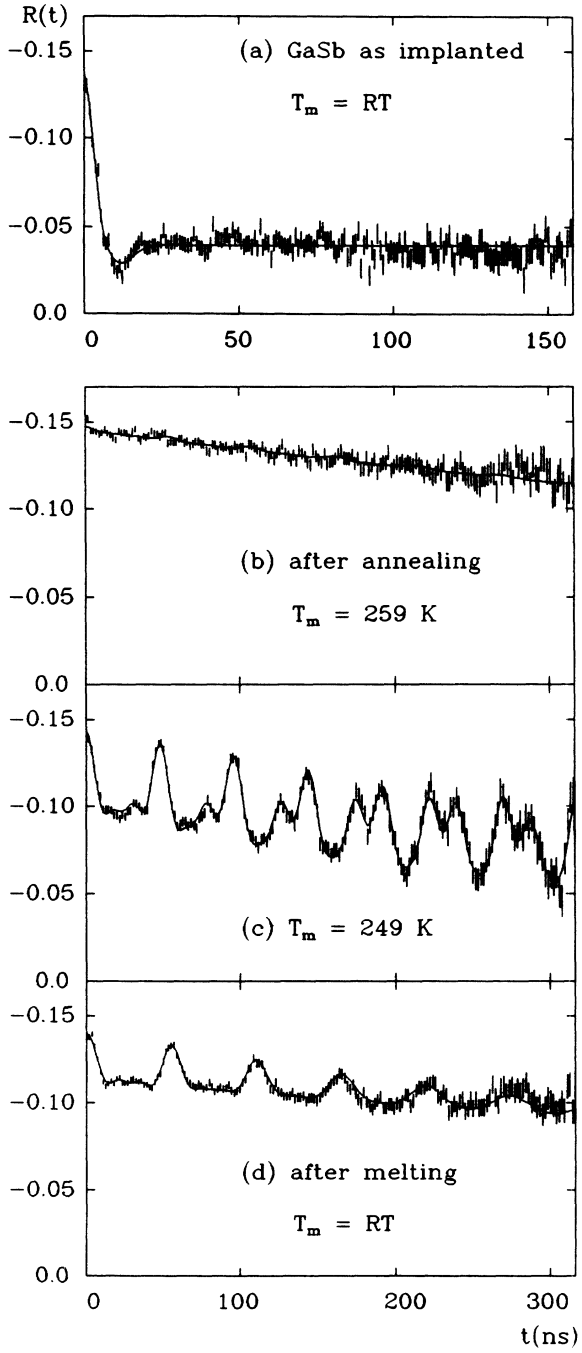

FIG. 4. TDPAC spectra of indium-implanted GaSb (a) as implanted; (b) after annealing, measured at 259 K; and (c) after annealing, measured at 249 K; and (d) after melting, measured at room temperature.

C. GaSb

The results obtained for GaSb are shown in Fig. 4. In this case, two components are necessary to describe the "as implanted" data. Beside the normal frequency distribution there is an unperturbed component (Table II). After annealing, in addition to the component which corresponds to Cd in zinc-blende lattice sites, we observed a fraction (32%) of the probes embedded in metallic gallium precipitates. The existence of this last component is evident at low temperatures, where gallium is frozen adopting the orthorhombic structure.

Such a spectrum is shown in Fig. 4(c). The well-defined component corresponds to an electric quadrupole interaction with $\eta=0.2$. This value is characteristic of the orthorhombic structure of gallium.[11] We have observed a temperature dependence of $T^{3/2}$ of the quadrupole frequency [Fig. 5(a)] and the slope $\mathcal{L}=1.4\times10^{-5}$ agrees with the value 1.45×10^{-5} reported for Cd in pure gallium.[11] The extrapolated value $\omega_Q(0)=23.10$ Mrad/s is also consistent with the data reported in the literature.

On the other hand, the gallium phase changes from liquid to solid between 260 and 250 K. The transition occurs 45° below the freezing point of gallium. In Fig. 6 it is shown how the physical state of the gallium phase,

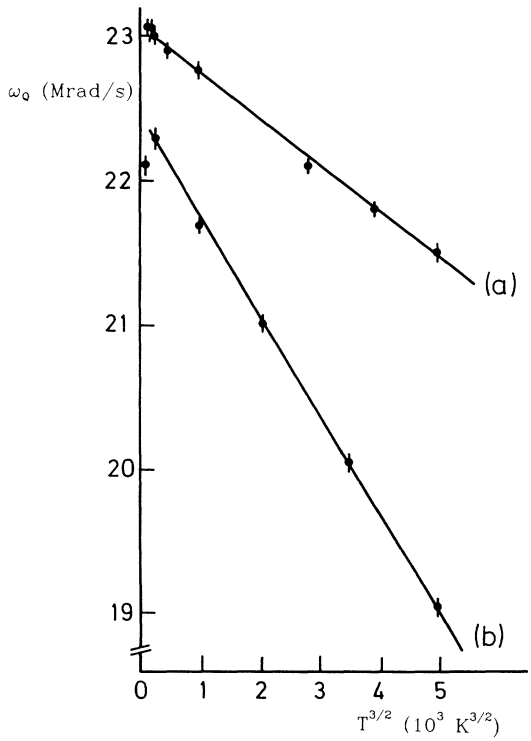

FIG. 5. Temperature dependence of the quadrupole interaction of ^{111}Cd in the (a) Ga-rich phase and (b) Sb-rich phase.

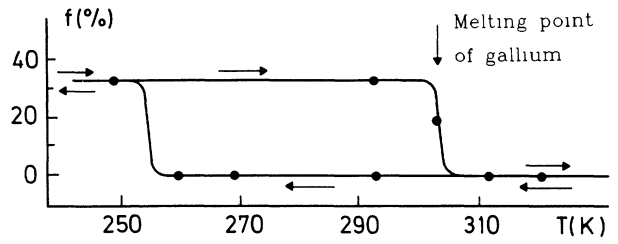

FIG. 6. Schematic plot illustrating the tendency of gallium to supercool below its freezing point. Shown is the fraction f of In probes in metallic Ga at different sample temperatures T. The arrows indicate the sense of the variations of T.

dispersed in GaSb, changes as a function of annealing temperature. The temperature of measurement was room temperature (RT) if the annealing treatment (10 min) was carried out at temperatures greater than RT. The arrows indicate the sense of change in the temperature. The process and its hysteresis can be connected with the known tendency of gallium to supercool below its freezing point. In a different experiment, we melted the sample after implantation. In this case a new component appears, besides that of Cd in zinc-blende structure. A typical spectrum is shown in Fig. 4(d). The temperature dependence of the quadrupole interaction is shown in Fig. 5(b). This quadrupole interaction is axially symmetric, depends on temperature with $T^{3/2}$ ($\mathcal{L}=3.0\times10^{-5}$), and the extrapolated value for $T=0$ is 22.46 Mrad/s. We assign this interaction to Cd probes in Sb-rich phases. This conclusion is obtained by comparing the present results with those reported by Barfuss *et al.*[12] for $Sb_{1-x}In_x$ alloys. From the slope of the straight line we can estimate a concentration of gallium of 0.2 wt. % in this phase. The location of indium in the Sb-rich phase can be explained by In and Sb precipitation in the melt.

In both experiments the component of indium in zinc-blende structure is well described by the perturbation factor given by Eq. (3). The λ values are similar in both cases and do not show a temperature dependence. In Fig. 2 we have plotted only the value measured at the lowest temperature. At the other temperatures we have obtained more or less the same value.

D. InSb

The results obtained for InSb are shown in Fig. 7. Like above, "as implanted" spectrum is fitted with two components (Table II). After annealing, all spectra can be fitted with expression (3) and the value of λ for the lowest temperature is shown in Fig. 2. No temperature dependence is observed.

E. AlSb

The results are shown in Fig. 8. Again two components are needed to fit the "as implanted" data (Table II). Upon heating this material shows a distinctively different behavior (Fig. 8). After annealing or melting a high fraction of probes are in sites without cubic symmetry. This fact can be attributed either to a high content of impurities (Table I) or to strong stoichiometric disturbances caused by the implantation. There is also no temperature dependence of the interaction.

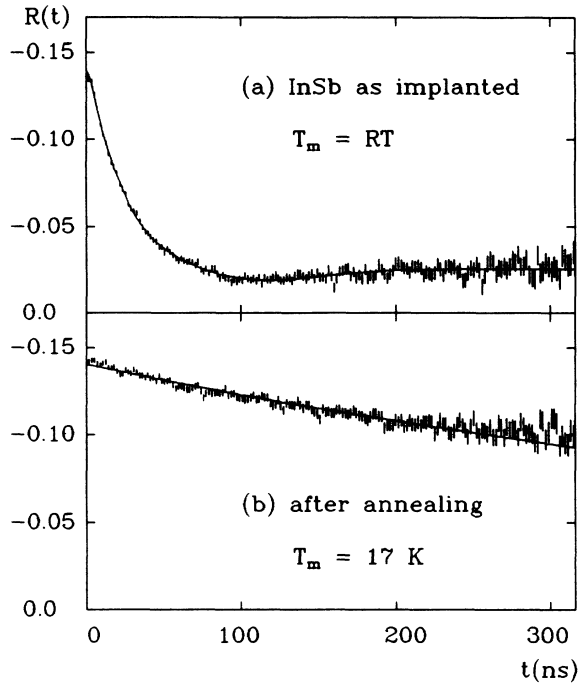

FIG. 7. TDPAC spectra of indium-implanted InSb (a) as implanted; (b) after annealing, measured at room temperature.

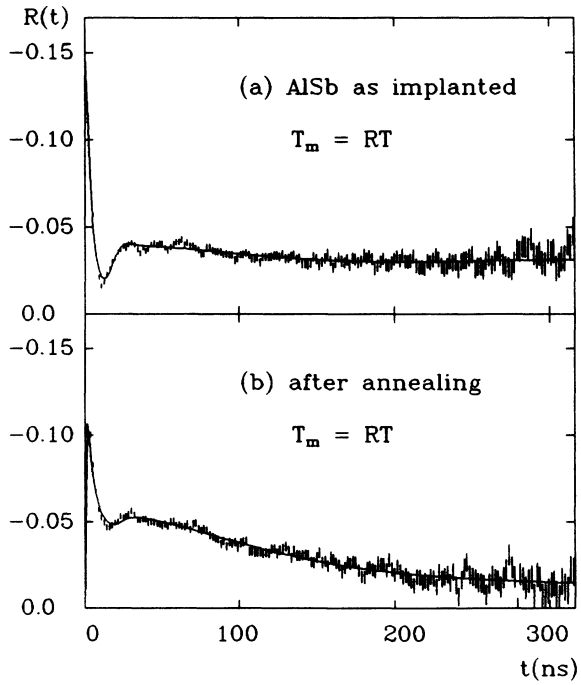

FIG. 8. TDPAC spectra of indium-implanted AlSb (a) as implanted and (b) after annealing, measured at room temperature.

IV. DISCUSSION

Due to a surrounding of cubic symmetry, a vanishing electric field gradient and therefore no quadrupole interaction is expected at a regular lattice site in semiconductors with diamond or zinc-blende structure. The strong reduction of the anisotropy observed in all samples before annealing is due to radiation damage caused by the implantation process. The corresponding hyperfine interaction parameters (Table II) show no definite trend with the mean atomic number of the constituents. However, the data indicate that implantation induced variations of the stoichiometry in the implanted region occur. The maximum value of ω_1 is reached for GaP with the largest mass ratio of the constituents and the largest mass differences to the projectile ^{111}In. The other extreme is InSb with nearly equal masses of constituents and projectile leading to the lowest value of ω_1. In the case of GaAs, although the mass difference to the projectile is large due to the similar masses of Ga and As, the stoichiometry is largely preserved.

In addition, it is worth mentioning that the presence of at least one constituent of a mass similar to the projectile favors the incorporation of ^{111}In on cubic lattice sites. This is indicated by the observation of an undisturbed fraction f_2 in AlSb and GaSb and most pronounced in InSb (Table II), where the probe is also a constituent of the host lattice.

After annealing, the average electric field gradient at the site of the probe atoms is close to zero. However, upon cooling the sample some increase of the average quadrupole interaction is observed. This could be caused by some lattice distortions around the impurity site which may be expected due to the following facts.

(i) The differences of the ionic radius and the atomic structure between the impurity ion and the host atoms cause local lattice distortions. This distortion may preserve the symmetry T_d, but favor the trapping of "electronic defects" that reduce the symmetry of the impurity surrounding.

(ii) The electron-capture decay of ^{111}In produces a highly ionized Cd ion with a recoil energy of 3 eV. Although this energy is very low as compared to the threshold energy for atomic displacement in semiconductors ($\sim$20 eV for elemental semiconductors and $\sim$10 eV for III-V compounds), the simultaneous occurrence of recoil energy, high ionization (resulting in a weakening of the bond energy), and lattice distortions (i) can result in permanent distortions at low temperature.

(iii) Although the electronic shells of the cadmium ion reach their ground state in a short time ($t < 1$ ns), the holes produced by the electron-capture decay may be bound to the distorted center, giving an additional source of an electric field gradient. Lampert[13] has predicted the existence of many hole-electron complexes which can be bound to impurities in semiconductors. Haynes[14] observed excitons bound to impurities in Si. More recently, bound exciton and multiexciton complexes associated with double acceptors in Ge have been reported.[15,16] A displacement of the acceptor resulting from the binding of a long lived complex has been observed in Ge:Zn.[17]

(iv) Distortion around the impurity can result from a Jahn-Teller effect. Such distortion occurs when the electronic state of the complex is degenerate, and its total energy can be reduced, by occupying the lowest split electronic level induced by the distortion.

Several experimental results have been explained by a Jahn-Teller distortion. Examples from the literature are Ge:Be (Ref. 18) (where the distortion occurs along $\langle 111 \rangle$ directions), Si:Al (Ref. 19) (trigonal distortion), and also hyperfine interaction results like Si:Cd$^-$,[3] Si:I,[20] Si:Pd,[21] Si:Pt,[21] and Ge:Ni.[22]

(v) Finally, it must be pointed out that the distorted configuration at low temperature at a Cd site could have memory of a distorted configuration around the In parent ion.

The temperature dependence of the relaxation parameter λ in the III-V compounds (Fig. 2) is much weaker than in the case of elemental semiconductors. This fact may be connected with the single acceptor nature of Cd in III-V hosts. The magnitude of the perturbation at low temperature decreases with increasing average atomic number of the host, showing a correlation between the magnitude of the effect and the weakening of the bonds between the valence electrons and the atomic nucleus. The decrease of λ, at a fixed temperature, is connected with a less pronounced distortion (a smaller average frequency) and a shorter correlation time, both facts being probably not independent. On the other hand, the correlation of the λ values with a particular physical property of the host lattice is not yet possible.

The higher fractional ionic character of the bonds in GaP seems to be insufficient to explain the higher λ values as compared to the other compounds. Probably they are connected with the already mentioned variation of the stoichiometry that produces two zones of different character in the material. The drop of λ at $T \sim 100$ K could indicate the ionization of some charged centers in the implanted regions.

We conclude that the results reported here are due to the existence of a distorted configuration around cadmium single acceptor impurities in III-V compounds. A better description of the distorted configuration is not possible at present. It seems to be difficult to decide on the relative importance of atomic displacement and the presence of holes in the distorted center. The same problem had been reported in the interpretation of infrared absorption spectra of Zn in Ge, where the experimental results have been explained either by bound excitons and bound multiexciton complexes associated with Zn (producing a displacement of the impurity)[17] or by a large acceptor ground-state splitting.[23]

ACKNOWLEDGMENTS

One of us (A.F.P.) acknowledges the support of the CICPBA-Argentine, the Alexander von Humboldt Foundation of the Federal Republic of Germany, and by the BMFT of the Federal Republic of Germany under Contract No. 03-B02B0N.

[1]A. F. Pasquevich and R. Vianden, Phys. Rev. B **35**, 1560 (1987).
[2]M. Deicher, G. Grübel, E. Recknagel, Th Wichert, and D. Forkel, Nucl. Instrum. Methods **13B**, 499 (1986).
[3]H. Kemerink, F. Pleiter, and M. Mohsen, Hyperfine Interact. **35**, 707 (1987).
[4]A. F. Pasquevich and R. Vianden, Phys. Rev. B **37**, 10 858 (1988).
[5]H. Wolf, S. Deubler, D. Forkel, M. Uhrmacher, F. Meyer, and W. Witthuhn, Mat. Sci. For. 38–41, 463 (1989).
[6]N. A. Goryunova, in *The Chemistry of Diamond Like Semiconductors,* edited by J. C. Anderson (Chapman and Hall, London, 1965).
[7]R. E. Avila and C. D. Fung, J. Appl. Phys. **60**, 1602 (1986).
[8]L. A. Mendoza Zelis, A. G. Bibiloni, M. C. Caracoche, A. Lopez Garcia, J. A. Martinez, R. C. Mercader, and A. F. Pasquevich, Hyperfine Interact. **3**, 315 (1977).
[9]A. Abragham and R. V. Pound, Phys. Rev. **92**, 943 (1953).
[10]M. Brüssler, H. Metzner, and E. Hunger, Hahn-Meitner Institut Annual Report No. 441, 1986 (unpublished), p. 122.
[11]W. Keppner, W. Körner, P. Heubes, and G. Schatz, Hyperfine Interact. **9**, 293 (1981).
[12]H. Barfuss, G. Böhnlein, F. Freunek, R. Hofmann, H. Hohenstein, W. Kreische, N. Niedrig, and A. Reimer, Hyperfine Interact. **10**, 967 (1981).
[13]M. A. Lampert, Phys. Rev. Lett. **1**, 450 (1958).
[14]J. R. Haynes, Phys. Rev. Lett. **4**, 31 (1960).
[15]H. Nakata and E. Otsuka, Phys. Rev. B **29**, 2347 (1984).
[16]R. Sauer and J. Weber, J. Phys. C **17**, 1421 (1984).
[17]H. Nakata and E. Otsuka, J. Phys. Soc. Jpn. **54**, 3605 (1985).
[18]W. J. Moore, Phys. Rev. B **29**, 7062 (1984).
[19]H. R. Chandrasekhar, A. K. Ramdas, and S. Rodriguez, Phys. Rev. B **12**, 5780 (1975).
[20]G. J. Kemerink, H. de Waard, L. Niesen, and D. O. Boerma, Hyperfine Interact. **14**, 53 (1983).
[21]H. H. Woodbury and G. W. Ludwig, Phys. Rev. **126**, 466 (1962).
[22]G. W. Ludwig and H. H. Woodbury, Phys. Rev. **113**, 1014 (1959).
[23]M. L. W. Thewalt, B. P. Clayman, and D. Labrie, Phys. Rev. B **32**, 2663 (1985).